Academic Science Journal

The Biological Activity of Green Synthesis ZnO Nanoparticles by *Citrus sinensis* Fruit Peels against *Staphylococcus aureus* isolated from Skin Infections

Thaka Hamza Aziz* and Abbas Yaseen Hasan

Department of Biology, College of Sciences, Diyala University, Iraq.

*thakaahamza@gmail.com

Received: 15 August 2023 **Accepted: 2 October 2023**

DOI: https://dx.doi.org/10.24237/ASJ.02.03.799B

Abstract

In this study, a green biological method was used to manufacture zinc oxide nanoparticles (ZnO NPs) from zinc nitrate as a precursor with an aqueous extract of *Citrus sinensis* fruit peels as reducing agents, when the color changed from yellow to brown, this indicates the production of ZnO NPs. The produced ZnO-NPs were characterized via X-ray diffraction (XRD), Fourier-Transform Infrared Spectroscopy (FTIR), Ultraviolet–visible spectroscopy (UV-Vis), and Atomic force -Microscopy (AFM). The synthesized ZnO-NPs have been characterized by the XRD peaks confirmed that the ZnO-NPs are hexagonal, and their purity and crystallinity are very high, with an average particle size of 16.21 nm. FTIR analysis was carried out to identify possible bio-molecules responsible for the bio-reduction of zinc ions.

Moreover, the surface plasmon resonance (SPR) measured at λmax = 378 nm, confirming the formation of ZnO-NPs. AEM images showed that ZnO-NPs have cubic morphology with sizes ranging from 50 nm. *Staphylococcus aureus* showed high resistance against Norfloxacin, Trimethprim, Ciprofloxacin, Levofloxacin, Clindamycin and Nirofuranation. The antibacterial effects of particles were investigated by agar well diffusion method using four concentrations of ZnO NPs (25, 50, 100, 200) mg/ml. The ZnO NPs showed the highest diameter of inhibition zone at 200 mg/ml concentration to *S.aureus* which was 25.5 mm, while the lowest diameter of inhibition zone was at (25) mg/ml concentration which was 15.4 mm. The minimum inhibitory

Academic Science Journal

concentration (MIC) of ZnO NPs was determined using a broth microdilution assay, which was 10.000 µg/ml on *S. aureus* isolates.

Keywords: *S. aureus*, ZnO NPs, *Citrus sinensis*, FTIR, UV-Vis.

الفاعلية الحيوية للتخليق الأخضر لاوكسيد الزنك النانوي بواسطة قشور فاكهة البرتقال ضد المكورات العنقودية الذهبية المعزولة من الاخماج الجلدية

ذكاء حمزة عزيز و عباس ياسين حسن

قسم علوم الحياة - كلية العلوم - جامعة ديالى

الخلاصة

في هذه الدراسة ، تم استخدام طريقة بيولوجية خضراء لتصنيع جزيئات أكسيد الزنك النانوية (ZnO NPs) من نترات الزنك كبوادئ مع مستخلص مائي من قشورفاكهة البرتقال كعوامل اختزال ، وتغير اللون من الأصفر إلى البني ، مما يشير إلى أن إنتاجZnO NPs . تم تحديد خصائصZnO NPs الناتجة عن طريق حيود الأشعة السينية (XRD) ، والتحليل الطيفي للأشعة تحت الحمراء (FTIR) ، والتحليل الطيفي المرئي فوق البنفسجي (UV-Vis) ، ومجهر القوة الذرية (AFM). تتميز ZnO-NPs المُصنَّعة بقمم XRD التي أكدت أن ZnO NPs سداسية ، ونقاوتها وبلورتها عالية جدًا ، بمتوسط حجم جسيمي يبلغ 16.21nm. تم إجراء تحليل FTIR لتحديد الجزيئات الحيوية المحتملة المسؤولة عن الاختزال الحيوي لأيونات الزنك. علاوة على ذلك، تم قياس رنين البلازمون السطحي (SPR) عند λmax = 378nm ، مما يؤكد تكوين ZnO-NPs. أظهرت صور AEM أن ZnO-NPs لها مورفولوجيا مكعبة بأحجام تتراوح من 50nm. أظهرت المكورات العنقودية الذهبية مقاومة عالية للنورفلوكساسين ، تريميثبريم ، سيبروفلوكساسين ، ليفوفلوكساسين ، كليندامايسين ونيروفورانيشن. درست التأثيرات المضادة للبكتيريا لجزيئات أوكسيد الزنك بواسطة طريقة الانتشار في الحفر بالاكار. واستخدمت أربعة تراكيز من جزيئات أوكسيد الزنك هي (25 ،50، 100، 200) ملغم / مل. أظهرت جزيئات أوكسيد الزنك أعلى قطر لمنطقة التثبيط بتركيز 200 ملغم / مل من بكتريا المكورات العنقودية الذهبية 25.5 مليمتر ، بينما أقل قطر لمنطقة التثبيط بتركيز 25 ملغم / مل 15.4 مليمتر. تم تحديد الحد الأدنى MIC للتركيز المثبط لجزيئات أوكسيد الزنك باستخدام طريقة التخافيف والذي كان 10.000 مايكروغرام / مل لعزلات المكورات العنقودية الذهبية.

الكلمات المفتاحية : المكورات العنقودية الذهبية, جزيئات أوكسيد الزنك ,نبات البرتقال, FTIR, UV-Vis .

Introduction

One of the most frequent reasons for the prescription of antibiotics in human medicine is for skin and soft tissue diseases, particularly pyoderma [1]. Regardless of the patient's age, the climate, or the patient's location, *Staphylococcus aureus* is the most frequent bacteria associated

with skin infections globally [2]. Gram-positive opportunistic pathogen *S. aureus* produces a range of infections in both nosocomial and community settings. Due to its greater ability to colonize and survive in many host tissues, *S. aureus* is a cause of a wide variety of diseases [3]. A handful of the bacteria's toxins that result in a wide range of clinical symptoms are thought to be responsible for the primary cutaneous clinical signs[4]. The primary toxins involved in the majority of dermatological symptoms linked to *S. aureus* include Panton Valentine leucocidin, exfoliatins, enterotoxins, and toxic shock syndrome toxin [5]. There is may be other, less common cutaneous symptoms in endocarditis and bacteremia. The most significant developed right now is the global spread of community-acquired *S. aureus* (CA-MRSA), which primarily causes skin infections such impetigo, folliculitis, furuncles, and primary abscesses [6]. *S. aureus* has acquired determinants through mobile genetic element horizontal gene transfer in order to develop resistance to numerous drugs [7]. Prior research has indicated that nanotechnology is a viable strategy for treating illnesses caused by microorganisms[8]. Nanoparticles (NPs) are being extensively researched for their potential antibacterial actions and offer a wide range of benefits[9]. Low cytotoxicity and a higher capacity to serve as drug delivery systems are characteristics of metallic oxide nanoparticles, such as Zinc oxide (ZnO NPs). It has been demonstrated that a variety of elements, including shape and surface charge, can significantly influence a nanomaterial's antibacterial characteristics[10] .ZnO NPs are less expensive and hazardous than other nanomaterials, making them suitable for use in a variety of anticancer, antibacterial, and anti-inflammation applications. In addition to their high catalytic efficiency, ZnO NPs also exhibit good adsorption capabilities and chemical stability[11]. An ideal substitute for harmful chemical reagents is the green production of ZnO NPs utilizing extracts of non-toxic natural plants. Acids, polyphenols, polysaccharides, terpenoids, flavonoids, and alkaloids are just a few of the phytochemicals found in natural plant extracts that make them effective reducing and stabilizing agents. *Citrus* sinensis peel extracts have so far been used to successfully manufacture ZnO nanoparticles [12] .One of the world's most productive fruits is *Citrus.* The primary by-product of *Citrus is*, *Citrus* peel, which is abundant in a range of natural antioxidants. In order to create ZnO NPs, *Citrus* peel extract is therefore thought to be used[13]. The study aimed to using *Citrus sinensis* fruit

peel extract for preparing ZnO NPs and determine their antibacterial activity against *S. aureus* which causes skin infections.

Materials and Methods

Bacterial Isolation

The present study involved 100 swabs were collected from clinical cases of cutaneous infection for both sex to identify gram-positive bacterial species (*S. aureus*) , which identified primarily by routine laboratory procedures which included the cultural media (blood agar and manitol salt agar) , microscopically morphology , biochemical tests (catalase and coagulase tests) [14], and diagnosed using Vitek2 (performed by BioMerieux Comp., France, 2019) tools in the bacteriology units at Baquba Teaching Hospital in Diyala and Medical City in Baghdad, Iraq during the period from the beginning of October 2022 to the end of January 2023 .

Antibiotics Susceptibility Testing

Using a Mueller-Hinton agar medium, the Kerby Bauer method was used to test antibiotic sensitivity on all isolates. The 12 antibiotics used in the current study were selected according to the clinical laboratory standards institute (CLSI,2023)[15], as depicted in Table 1. The diameters of the zones, including the zone of inhibition, were measured and recorded in millimeters after incubating overnight at a temperature of 37˚C. These measurements were then compared with the standard inhibition zone[16].

Table 1: The antibiotics discs used in this study

Antibiotics disc	Symbol	Disc con (µg/ml)
Chloramphenicol	C	30
Ciprofloxacin	CIP	5
Clindamycin	CD	2
Gentamicin	GM	10
Imipenem	IMI	30
Levofloxacin	LEV	5
Meropenem	MEM	10
Nirofuranation	NIT	300
Norfloxacin	NOR	10
Tetracyclin	T	30
Trimethprim	TR	15
Vancomycin	VA	30

Biosynthesis of ZnO-NPs from *Citrus sinensis*

The synthesis of zinc oxide nanoparticles (Zn-NPs) was conducted by the method described by Gao *et al*.[17]. A quantity of two grams of zinc nitrate with a purity of 99% was dissolved in a container holding 85 milliliters of deionized distilled water (D.W). The resulting solution was then agitated for 15, minutes; after which it was combined with 50 milliliters of *Citrus sinensis peel*. Subsequently, the mixtures were stirred for 60 minutes and subjected to a water bath maintained at 60°C for 60 minutes. Following this, the combinations dried at 150°C, followed by a subsequent heat treatment at 400°C for one hour. The chemical compounds in orange peel extract, namely flavonoids, limonoids, and carotenoids, function as ligands. The hydroxyl aromatic ring groups, which are among the extract's constituents, can create intricate ligands with zinc ions. Nanoparticles are stabilized and formed through the sequential stages of nucleation and shape. The organic solution combination is subsequently subjected to direct decomposition through calcination at a temperature of 400°C, leading to the liberation of ZnO-NPs[18].

Characterizations of ZnO-NPs

The crystallinity of the dried ZnO nanoparticles was characterized using X-ray diffraction (XRD) analysis using Siemens D5000 equipment (Bruker, Germany). Fourier transform infrared spectroscopy (FTIR) analysis detected the vibrational peaks of the ZnO nanoparticles, employing a Tensor 27 equipment manufactured by Bruker. The presence of ZnO nanoparticles (NPs) was verified by measuring their wavelength in the UV-VIS spectrum using a UV-2450 spectrophotometer manufactured by Shimadzu in Japan. The dimensions, surface texture, and volume of the ZnO nanoparticles were analyzed using Atomic Force Microscopy (AFM)[19]. The experiments were conducted at the Ministry of Higher Education and Scientific Research in Iraq.

Anti-bacterial activity of ZnO NPs for agar diffusion test

The antibacterial efficacy of the synthesized ZnO NPs was evaluated against *S. aureus* isolates. This assessment was conducted by the agar well diffusion test, following the established Kirby-Bauer methodology[20]. The ZnO NPs were inoculated with a previously cultured bacterial

strain for 24 hours. This was achieved by employing a sterilized cotton swab plunged into the broth containing these bacterial cultures. Following the solidification of 20 ml of Mueller Hinton agar in Petri plates, wells were created using a sterilized cork borer with a diameter of 8 mm. A 100 µl suspension containing ZnO NPs at different concentrations (25, 50, 100, and 200 mg/ml) was added to the respective wells. The bacterial suspensions were compared to a standard MacFarland solution with a concentration of 1.5 x 10^8 colony-forming units per milliliter (CFU/ml). The Petri dishes were incubated at 37°C for 24 hours in the incubator. The ZnO NPs efficacy against bacteria was assessed by quantifying the bacterial zone of inhibition (measured in millimeters)[21]. The minimum inhibitory concentration (MIC) of the synthesised ZnO NPs was assessed against *S. aureus* using the two-fold macro broth dilution method, as described by Fahad *et al*.[22]. The experiment commenced by utilising *S. aureus* colonies obtained from nutrient agar plates that had been incubated overnight to inoculate the broth. A freshly prepared culture of *S. aureus*, with a concentration of 2 × 106 colony-forming units per milliliter (CFU/mL), was utilised to inoculate individual tubes. These tubes were subjected to a two-fold serial dilution process using ZnO NPs at various concentrations (5000, 10000, and 20000 µg/mL).

Results and Discussion

Bacterial isolation and identification

The positive growth samples were 95 from a total of 100 samples distributed between (70%) *S. aureus*, (15%) *Pseudomonas aeruginosa*, (5%) *E.coli* and (5%) *S. epidermidis*, while 5 samples showed no growth as appeared in figure (1).

Academic Science Journal

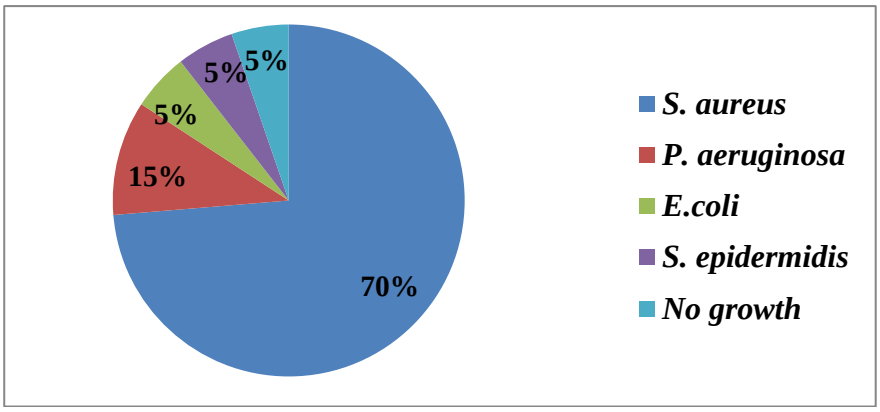

Figure 1: The percentage of isolated bacteria from cutaneous infections

These results agree with a study done in Iraq by Jawad [23], which showed 50% of *S. aureus* isolated from cutaneous infection. Mohammed and Flayyih[24], recorded that 55% isolates from wounds were identified as *S. aureus*,but the results of our study are incompatible with study performed in Baghdad by Al-Saleh *et al*.[25], which recorded that 45% isolates that isolated from abscesses were identified as *S. aureus*. *S. aureius* is a significant etiological agent responsible for a variety of infections, encompassing both superficial skin infections and more severe manifestations including hair follicle abscesses, deep tissue infections, and systemic infections affecting vital organs such as the lungs, blood, and bones[26]. Recent studies conducted in the local area have documented the identification and isolation of *S. aureius* from various clinical specimens. Hassan [27].documented that 55% of the total isolates were identified as *S. aureius*.. The current results in figure (2) shows males were more infected with *S. aureius* than females 65% and 35% respectively.

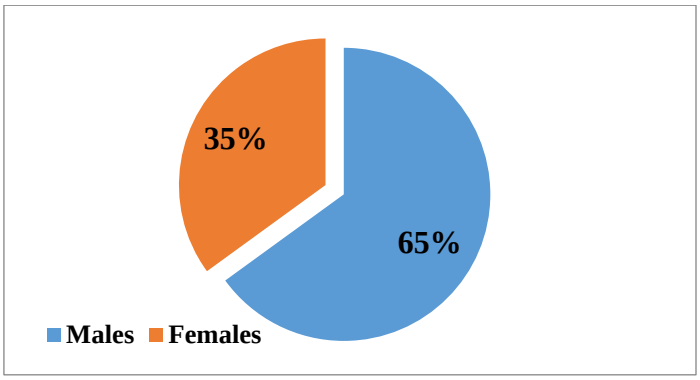

Figure 2: Distribution of *S. aureus* isolates according to gender

The effect of sex on the *S. aureus* carriage rate was studied previously in Iraq in a community setting. A study done in Iraq by, Aljboori *et al.[28]*, who showed a higher rate of infection with *S. aureus* in males 61% compared with females 39% ; In a separate investigation conducted by Menard et al.[29], it was observed that the prevalence of skin infection carriage was higher among females compared to males. However, the variance did not reach a statistically significant level. A study conducted in Palestine yielded similar findings, indicating a greater carriage rate of *S. aurieus* infection in males compared to females[30], nor correlation was reported between the sex of the admitted patients and the isolation rate of *S. aureus* in Iraq.

Antimicrobial Susceptibility Testing

The susceptibility test was done for all *S. aureus* isolates by disk diffusion method to examine 12 different antibiotics. The isolates were resistance 87% to Norfloxacin, 87% to Trimethprim, 85% to Ciprofloxacin, 78% to Levofloxacin, 77% to Clindamycin, 77% to Nirofuranation ,75% to Chloramphenicol, 75% to Gentamicin, 75% to Tetracyclin, 69% to Imipenem, 65% to Meropenem, and 35% to Vancomycin, figure (3) .

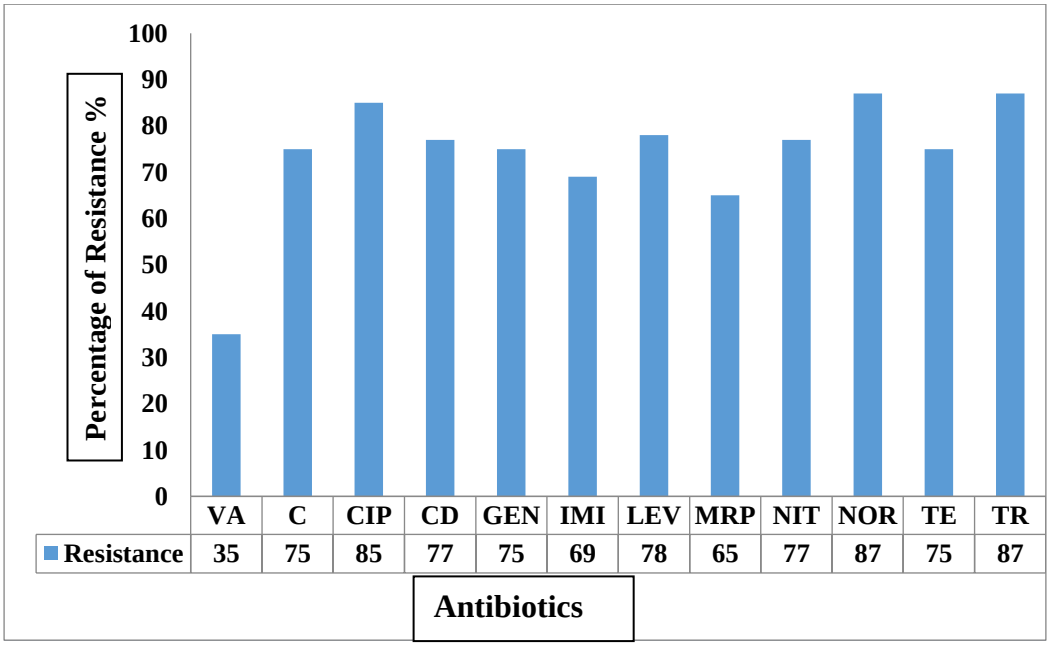

Figure 3: Resistance of *S.aureus* to the antibiotis :

Chloramphenicol (C), Ciprofloxacin (CIP), Clindamycin (CD), Gentamicin (GEN), Imipenem (IMI), Levofloxacin (LEV), Meropenem (MRP), Nirofuranation (NIT),Norfloxacin (NOR), Tetracyclin (TE),Trimethprim (TR) , Vancomycin (VA).

S. aurieus isolates showed high resistance towards most antimicrobia1 agents that have been tested. In a study carried out by Doha and Lagoon [31]which performed on 74 *S. aurieus* isolates collected from hospitalized patients in Baghdad, the results showed percentage of isolates resistance towards Tetracycline , Vancomycin, Ciprofloxacin and Gentamicin were 70% , 31% , 16.4%, and 13.11% respectively , this results agreed to some extent with the results of the current study in relation to Vancomycin and Ciprzofloxacin resistance but disagreed in the case of Ciprofloxacin and Gentamicin resistance. Staphylococci resist tetracycline, through two mechanisms: first, active efflux of the antibiotic; second, the ribosome to the drug. Tet (K) is the major gene in Staphylococci that encoding active efflux[32].

In a study done by Afshari[33], the results showed highly resistance of *S.aureus* isolates which collected from hospitalized patients against Trimethprim (85%) and Levofloxacin (82%), this results agreed with the present study . In resistant strains an enzyme called beta-lactamase is present which serves to 'break' the beta lactam ring, which effectively nullifies the antibiotic's effectiveness, *S. aureus* which classically produce penicillinase as well as cephalosporinase that destroy the antibacterial agent before it can have an effect[34].

Green Synthesis of ZnO-NPs from *Citrus sinensis* extract

ZnO -NPs were prepared according to Hajiashrafi *et al.* [35]. Aqueous extracts of *Citrus sinensis* peel have been used to biosynthesize ZnO-NPs. *Citrus* extracts contain several compounds, such as carotenoids, minerals, essential oil, folic acid, and alkaloids. These alkaloids operate as reduction agents for Zinc acetate, facilitating the synthesis of ZnO -NPs. The phenolic composite demonstrates significant antioxidant properties, making it an effective agent for reducing metal particles and facilitating the creation of environmentally friendly nanoparticles. The primary method for assessing the synthesis of nanoparticles, as depicted in

Figure 4, involves observing color changes. Specifically, the transition to a pale-yellow hue serves as an indicative sign of ZnOi-NPs development.[17].

Figure 4: Synthesis of ZnO nanoparticles by *Citrus sinensis* fruit peels

Characterization of ZnO-NPs

X-ray Diffraction (XRD) Analysis

XRD is an expeditious analytical method for identifying crystalline material phases. The X-ray diffraction pattern of ZnO nanopowder is depicted in Figure 5. The XRD investigation yielded data on peak intensity, position, width, and the entire width of the peaks at half-maximum (FWHM). The diffraction peaks observed at specific angles, namely 31.7 ° (100), 34.4 ° (002), 47.5 ° (102), 56.5 ° (110), 62.8 ° (103), and 67.96 (112), were found to be consistent with the hexagonal wurtzite phase of ZnO, as indicated by the Joint Committee on Powder Diffraction Standards (JCPDS card number: 36-1451). These peaks were successfully indexed and matched the expected pattern for ZnO [36]. The absence of any characteristic XRD peaks other than those associated with ZnO confirms that the synthesized nanopowder was free from impurities. The synthesized ZnO -NPs' diameter was determined using the Debye-Scherrer formula $D = 0.9 \lambda / \beta \cos \theta$[37]. This study found that the average grain size of the sample was 16.21 nm, and the result of this study was similar to that reported by Abdel-Khaleq and Al-Askar[38], who recorded an average size of 15 nm.

Academic Science Journal

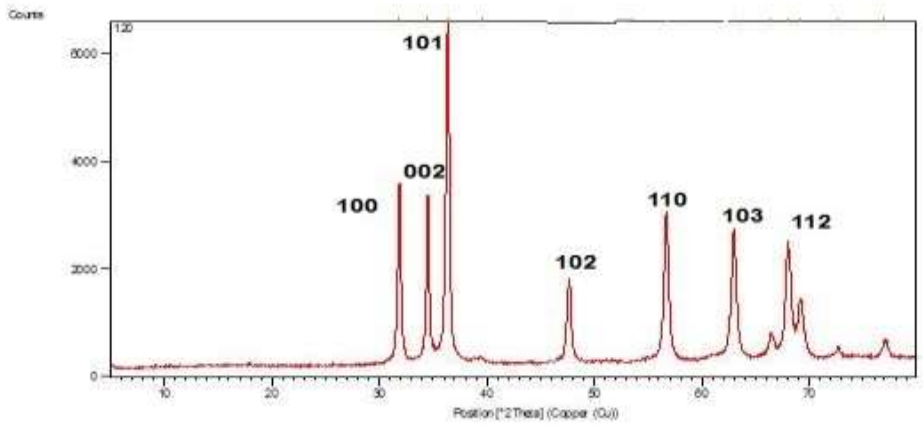

Figure 5: XRD pattern of prepared ZnO-NPs

Fourier-Transform Infrared Spectroscopy (FTIR) Analysis

FTIR spectroscopy was used to find the functional groups in the *Citrus sinensis* extract that could act as reducing agents in making ZnO-NPs. This study found that zinc acetate dihydrate was changed into ZnO-NPs by the secondary metabolites of *Citrus sinensis*. Biosynthesized ZnO-NPs had several peaks in their FTIR spectrum at 3537.9, 2825.7, 1495.9, 1383.7, 1255.5, 1118.1, 1005.3, 863.3,776.8,700.6, and 575.9 cm^{-1} figure (6). The broad peak at 3245 cm^{-1} showed that there were hydrogen-bonded groups, which could be hydroxyl groups (O-H) extending from the phenolic compounds in the plant extract[39]. In the same way, the peaks at 3537.9 cm^{-1} show that the O-H group is stretching[40]. The N–H bond of the primary and secondary amides was found in the band at 2825.7. The peaks at 1495.9, 1383.7, 1255.5, and 1118.1 cm^{-1} are due to a C=C stretch of alkenes or a C=O stretch of amides[41]. The bands at 1005.3 cm^{-1} are thought to be caused by proteins in the leaf extract that stretched the C-O bond when they moved. Also, peaks at 863.3,776.8, and 700.6 cm^{-1} could be due to amine groups with stretching C-N bonds. The Zn-O bond was found to have the essential absorption band at 575.9 cm^{-1} [42].

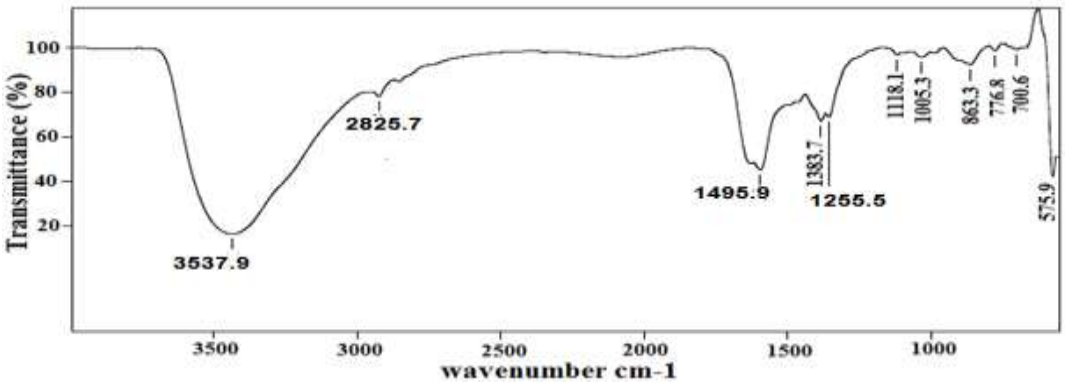

Figure 6: FTIR spectra of ZnO-NPs bio-synthesized by *Citrus sinensis*

UV-visible Analysis

UV-visible spectroscopy was used to show that ZnO NPs were made by biosynthesis. The color of the reaction ranged from clear to white. The color change indicates that ZnO nanoparticles are being made, as shown by the UV visual spectra. Figure 7. The sharp peak at 378 nm showed ZnO NPs in the mixture. The electronic cloud's movement on the ZnO NPs' general skeleton may be to blame for the wide absorption band that gets wider as the wavelength gets longer. This result is in agreement with a study done by Nazir *et al.* [43], who recorded that the ZnO absorption peak was 375nm.

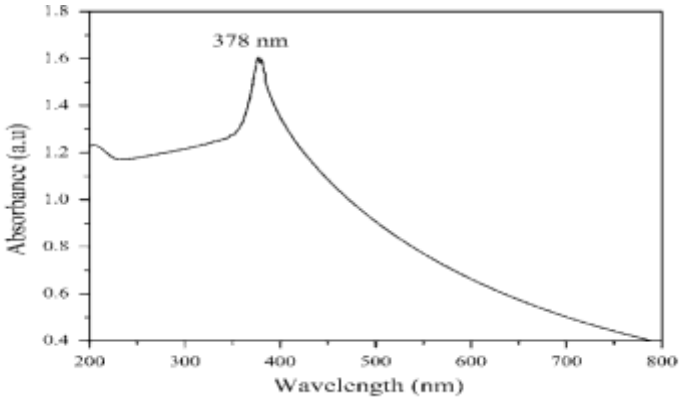

Figure 7: UV-Vis spectrum of synthesized ZnO-NPs by *Citrus sinensis*

Atomic Force Microscopy (AFM)

The AFM was used to distinguish the surface morphology and to define topography which provides 2D and 3D of AFM NPs surface images at an atomic level with the conforming size

distribution of ZnO-NPs. The average particle diameter size is 50 nm which was calculated in nano-scale size, Figure (8)**.** The images from AFM showed rotational ellipsoidal and cubic shapes of NPs, the present results agree with Torres-Rivero *et al.[44]*.

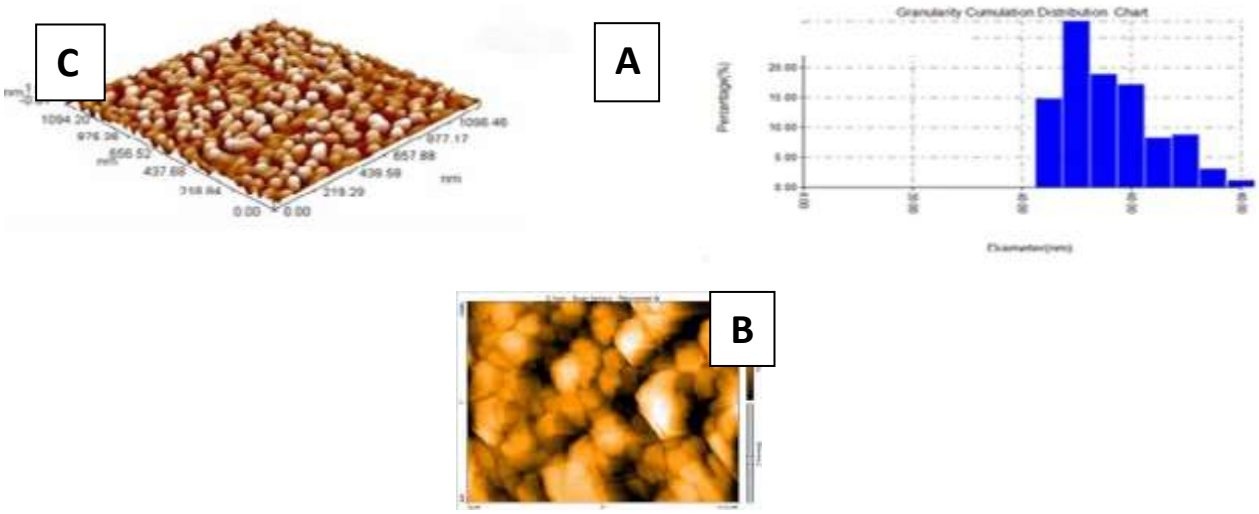

Figure 8: Biosynthesized ZnO-NPs by *Citrus sinensis* **(A)** Granularity Distribution Chart of ZnO -NPs synthesis **(B)** 2D image of ZnO-NPs **(C)** 3D image of ZnO-NPs synthesis.

Antibacterial activity of ZnO-NPs against *S. aureus*

The ZnO-NPs presented a remarkably antibacterial effect against *S. aureus* isolates (multidrug-resistance) as shown in table (2). The ZnO NPs showed the highest diameter of inhibition zone at concentration 200 mg/ml of *S.aureus* is 25.5 mm, while the lowest diameter of inhibition zone at concentration 25 mg/ml is 15.4 mm. This results were close to Gao *et al.* [17].

Table 2: Shows the Effect of ZnO NPs on *S. aureus* (zones of inhibition)

Concentrations (mg\ml)	**Inhibition Zone Mean ±St.Error**
25	15.4 ± 0.208
50	21.6 ± 0.212
100	23.3 ± 0.173
200	25.5 ± 0.251

The findings derived from the disc diffusion method indicated that the presence of starch-based ZnO-NPs at various doses exhibited inhibitory properties against *S. aureus* isolates. The present study involved the reduction of aqueous Zn^{+2} to ZnO-NPs through the use of plant extracts obtained from *Citrus sinensis*. The hypothesised mechanism for the reduction of Zn^{+2} to ZnO-NPs involves the interaction of biological substances present in plant extracts and their functional groups with the reaction mixture. The results of our study are agreement with the study conducted by Alamdari [39] who indicated the highest diameter of inhibition zone at concentration 200 mg/ml against *S.aureus* isolates. Studies on the antibacterial Behavior of ZnO NPs have shown that the morphology and oxidative stress play important roles in the antibacterial activity[45, 46]. The antibacterial activity of ZnO-NPs can be attributed to several mechanisms. Firstly, the generation of reactive oxygen species (ROS) plays a crucial role. Secondly, when ZnO-NPs come into contact with the cell wall, it leads to the loss of cellular integrity. Lastly, the release of Zn+2 ions also contributes to the antibacterial effect[47, 48]. The generation of ROS by metal oxide nanoparticles (MNPs) is a frequently documented mechanism underlying antibacterial action in the scientific literature [48, 49]

Determination of MIC by broth serial dilution method of ZnO NPs

Nanotechnology offers a viable approach for the development of new antimicrobial drugs, which have the capability to effectively eradicate bacterial cells. Moreover, nanotechnology exhibits significant promise for application in both medical and veterinary applications. The inhibitory effects of different concentrations of ZnO NPs on *S. aureus* isolates. MIC of ZnO NPs is (10000 µg/ml) on *S. aureus* isolates. The results of this study are consistent with previous report by Albukhaty *et al[46]*.The results of current study were agreement with a study in Iraq conducted by Al-Mosawi *et al.* [47]that showed high effectively of ZnO NPs against *S.aureus* isolates because of the difference in charge between bacteria and nanoparticles and inhibition of permeability of cell membrane then cell dead.

A study done by Jasim *et al.* [48]ZnO NPs are widely used to inhibit bacterial growth of pathogenic bacteria that resist certain antibiotics. It has been approved that ZnO NPs have a distinct potential against *S. aureus* strains exhibited resistance to methicillin (MRSA).

Conclusions

Staphylococcus aureus is a Gram-positive bacterium and commensal microorganism that colonizes about 50% of the anterior nares of human individuals.UV-Vis, XRD, FTIR, AFM analysis showed the crystalline organization, spherical shape of ZnO NPs .This study showed that the efficiency of ZnO NPs against *S.aureus* isolates (multidrug-resistant bacteria) is higher than other antibiotics that used in the study.

References

1. S. S. Costa, Staphylococcus aureus causing skin and soft tissue infections in companion animals: Antimicrobial resistance profiles and clonal lineages, Antibiotics, 11(5),599(2022)
2. A. Salmanov, Nosocomial transmission of multi-drug-resistant organisms in Ukrainian hospitals: results of a multi-centre study (2019–2021), Journal of Hospital Infection, 132,104-115(2023)
3. R. Leistner, Skin Infections Due to Panton-Valentine Leukocidin–Producing S. Aureus, Deutsches Ärzteblatt International, 119(45), 775(2022)
4. B. Silverberg, A structured approach to skin and soft tissue infections (SSTIs) in an ambulatory setting, Clinics and Practice, 11(1), 65-74(2021)
5. D. Gupta, Bacterial skin and soft tissue infections in children, Pediatr Inf Dis, 3,147(2021)
6. N. Tsouklidis, Understanding the fight against resistance: hospital-acquired methicillin-resistant Staphylococcus aureus vs. community-acquired methicillin-resistant Staphylococcus aureus, Cureus, 12(6), (2020)
7. A. Bitrus, Staphylococcus aureus: A review of antimicrobial resistance mechanisms, Veterinary Sciences: Research and Reviews, 4(2), 43-54(2018)
8. V. P. Jain, Advanced functionalized nanographene oxide as a biomedical agent for drug delivery and anti-cancerous therapy: a review, European Polymer Journal, 142, 110124(2021)

9. A. W. Alshameri, M. Owais, *A*ntibacterial and cytotoxic potency of the plant-mediated synthesis of metallic nanoparticles Ag NPs and ZnO NPs: A Review, OpenNano, 100077(2022)
10. A. Abdelghafar, N. Yousef, M. Askoura, Zinc oxide nanoparticles reduce biofilm formation, synergize antibiotics action and attenuate Staphylococcus aureus virulence in host; an important message to clinicians, BMC microbiology, 22(1),1-17(2022)
11. S. M. El-Megharbel, Utilizing of (zinc oxide nano-spray) for disinfection against "SARS-CoV-2" and testing its biological effectiveness on some biochemical parameters during (COVID-19 pandemic), ZnO nanoparticles have antiviral activity against (SARS-CoV-2), Coatings, 11(4), 388(2021)
12. J. Singh, Green'synthesis of metals and their oxide nanoparticles: applications for environmental remediation, Journal of nanobiotechnology, 16(1),1-24(2018)
13. B. Singh, Insights into the chemical composition and bioactivities of citrus peel essential oils, Food Research International, 143, 110231(2021)
14. S. Y. Tong, Staphylococcus aureus infections: epidemiology, pathophysiology, clinical manifestations, and management, Clinical microbiology reviews, 28(3), 603-661(2015)
15. W. C. FR, Performance standards for antimicrobial susceptibility testing; twenty-second informational supplement, Clinical and Laboratory Standards Institute, 32,M100(2023)
16. M. M. Al-Jebouri, S. A. Mdish, Antibiotic resistance pattern of bacteria isolated from patients of urinary tract infections in Iraq, (2013)
17. Y. Gao, Green synthesis of zinc oxide nanoparticles using Citrus sinensis peel extract and application to strawberry preservation: A comparison study, Lwt, 126, 109297(2020)
18. T. U. D. Thi, Green synthesis of ZnO nanoparticles using orange fruit peel extract for antibacterial activities, RSC advances, 10(40), 23899-23907(2020)
19. M. Azarang, Synthesis and characterization of ZnO NPs/reduced graphene oxide nanocomposite prepared in gelatin medium as highly efficient photo-degradation of MB, Ceramics International, 40(7), 10217-10221(2014)

20. M. Alekish, In vitro antibacterial effects of zinc oxide nanoparticles on multiple drug-resistant strains of Staphylococcus aureus and Escherichia coli: An alternative approach for antibacterial therapy of mastitis in sheep, Veterinary world, 11(10),1428(2018)
21. Y. T. Chung, Synthesis of minimal-size ZnO nanoparticles through sol–gel method: Taguchi design optimisation, Materials & Design, 87, 780-787(2015)
22. N. D. Fahad, Surface modification of hybrid composite multilayers spin cold spraying for biomedical duplex stainless steel, Heliyon, 9(3),(2023)
23. A. A. Jawad, A. A. Mohammed, A. Al-Hashimi, Epidemiological Study on the Prevalence of Staphylococcus aureus PVL Gene Among Healthy Community in Al-Karkh and Al-Rusaffa Districts Baghdad, Iraq, Iraqi Journal of Science, 441-448(2022)
24. A. J. Mohammad, M.T. Flayyih, I. B. Falih, Antibacterial Effect Of Arabic Coffee Extract Against Experimentally Infection With E, Coli In Mice, Biochemical & Cellular Archives, 22(1),(2022)
25. A. Al-Saleh, Trends in methicillin-resistant Staphylococcus aureus in the Gulf Cooperation Council countries: antibiotic resistance, virulence factors and emerging
26. M. S. Linz, Clinical Impact of Staphylococcus aureus Skin and Soft Tissue Infections, Antibiotics, 12(3), 557(2023)
27. H. Hassan, Heat resistance of Staphylococcus aureus, Salmonella sp., and Escherichia coli isolated from frequently consumed foods in the Lebanese market, International Journal of Food Properties, 25(1), 2435-2444(2022)
28. M. M. Aljboori, R. A. Abdul-Jabbar, A. I. A. Al-Ezzy, Evaluation of risk factors for infection with s. Aureus and mrsa among patients admitted to al-batool teaching hospital for maternity and children in diyala, iraq, Evaluation, 140(05),(2022)
29. G. Menard, Clustered cases of infections due to an uncommon methicillin-resistant Staphylococcus aureus originating in a maternity ward, Infectious diseases now, 51(6), 540-546(2021)
30. F. Damato, P. Ricci, S. Ricci, Correlations Between Roschach And Wais-Iv In Subjects With Intellectual Disability, Istisan Congressi, 58-58(2021)

31. Q. R. C. Doha, W. B. Lagoon, International Congress on Pathogens at the Human-Animal Interface (ICOPHAI), Abstracts Day, 1,24(2017)
32. J. Stephen, The major facilitator superfamily and antimicrobial resistance efflux pumps of the ESKAPEE pathogen staphylococcus aureus, Antibiotics, 12(2), 343(2023)
33. A. Afshari, Methicillin-and vancomycin-resistant Staphylococcus aureus and vancomycin-resistant enterococci isolated from hospital foods: Prevalence and antimicrobial resistance patterns, Current Microbiology, 79(11), 326(2022)
34. G. da Costa de Souza, C. A. Roque-Borda, F. R. Pavan, Beta-lactam resistance and the effectiveness of antimicrobial peptides against KPC-producing bacteria, Drug Development Research, 83(7),1534-1554(2022)
35. S. Hajiashrafi, N. Motakef-Kazemi, Green synthesis of zinc oxide nanoparticles using parsley extract, Nanomedicine Research Journal, 3(1), 44-50(2018)
36. W. Elmer, J. C. White, The future of nanotechnology in plant pathology, Annual review of phytopathology, 56,111-133(2018)
37. N. J. Alaallah, Eco-friendly approach for silver nanoparticles synthesis from lemon extract and their anti-oxidant, anti-bacterial, and anti-cancer activities, Journal of the Turkish Chemical Society Section A: Chemistry, 10(1), 205-216(2023)
38. A. Abdelkhalek, A. A. Al-Askar, *G*reen synthesized ZnO nanoparticles mediated by Mentha spicata extract induce plant systemic resistance against Tobacco mosaic virus, Applied Sciences, 10(15), 5054(2020)
39. S. Alamdari, Preparation and characterization of zinc oxide nanoparticles using leaf extract of Sambucus ebulus, Applied Sciences, 10(10), 3620(2020)
40. R. Mohammadi-Aloucheh, Green synthesis of ZnO and ZnO/CuO nanocomposites in Mentha longifolia leaf extract: characterization and their application as anti-bacterial agents, Journal of Materials Science, Materials in Electronics, 29,13596-13605(2018)
41. F. Erci, R. Cakir-Koc, I. Isildak, Green synthesis of silver nanoparticles using Thymbra spicata L. var. spicata (zahter) aqueous leaf extract and evaluation of their morphology-dependent antibacterial and cytotoxic activity. Artificial cells, nanomedicine, and biotechnology, 46(sup1),150-158(2018)

42. S. Vijayakumar, Biosynthesis, characterization and antimicrobial activities of zinc oxide nanoparticles from leaf extract of Glycosmis pentaphylla (Retz.) DC. Microbial pathogenesis, 116, 44-48(2018)
43. A. Nazir, Zinc oxide nanoparticles fabrication using Eriobotrya japonica leaves extract: Photocatalytic performance and antibacterial activity evaluation, Arabian Journal of Chemistry, 14(8), 103251(2021)
44. K. Torres-Rivero, Metal and metal oxide nanoparticles: an integrated perspective of the green synthesis methods by natural products and waste valorization: applications and challenges, Comprehensive analytical chemistry, 94 433-469(2021)
45. S. Banerjee, Antibacterial, anti-biofilm activity and mechanism of action of pancreatin doped zinc oxide nanoparticles against methicillin resistant Staphylococcus aureus, Colloids and surfaces B: Biointerfaces, 190, 110921(2020)
46. A. Bukhari, Green synthesis of metal and metal oxide nanoparticles using different plants parts for antimicrobial activity and anticancer activity: a review article, Coatings, 11(11), 1374(2021)
47. K. K. Shah, Assessment of Antimicrobial activity of novel zinc oxide nanoparticles synthesized through coffee bean and xylitol formulation against oral pathogens, Journal of Population Therapeutics and Clinical Pharmacology, 30(15), 381-386(2023)
48. E. Ren, Leveraging metal oxide nanoparticles for bacteria tracing and eradicating, View, 1(3),20200052(2020)
49. S. Albukhaty, H. Al-Karagoly, M. A. Dragh, Synthesis of zinc oxide nanoparticles and evaluated its activity against bacterial isolates, J. Biotech Res, 11, 47-53(2020)